



# Influences of changing sea ice and snow thicknesses on Arctic winter heat fluxes

Laura Landrum<sup>1</sup>, Marika M Holland<sup>1</sup>

<sup>1</sup>National Center for Atmospheric Research, Boulder, CO, USA

5 *Correspondence to:* Laura Landrum (landrum@ucar.edu)

**Abstract.** In the high latitude Arctic, wintertime sea ice and snow insulate the relatively warmer ocean from the colder atmosphere. As the climate warms, wintertime Arctic surface heat fluxes will be dominated by the insulating effect of snow and sea-ice covering the ocean until the sea ice thins enough or sea ice concentrations decrease enough such that direct ocean-atmosphere heat fluxes become more important. Simulated wintertime conductive heat fluxes in the ice-covered Arctic Ocean increase ~7-11 W m<sup>-2</sup> by mid-21<sup>st</sup> century and are due to both thinning sea ice and snow on sea ice. Surface heat flux estimates calculated using grid-cell mean values of sea ice thicknesses underestimate mean heat fluxes by ~16-35% and overestimate changes in conductive heat fluxes by up to ~36% in the wintertime Arctic basin even while sea ice concentrations remain above 90%.

## 1 Introduction

15 The Arctic is warming rapidly, and much more rapidly than lower latitudes. This Arctic amplification (AA) is due to a combination of a number of related mechanisms, including sea ice loss, lapse rate and Plank feedbacks, and changing water vapor and clouds, among others (e.g. Graverson and Wang, 2009; Kumar et al, 2010; Screen et al., 2013; Pithan and Mauritsen, 2014; Vavrus, 2004; Feldl et al., 2020). Sea ice loss contributes to increased surface warming through two primary methods: an albedo feedback, and an insulating effect. The albedo feedback results from sea ice concentration losses that expose dark ocean water and sea ice surface state changes, including reduced snow cover and increased ponding, that darken the ice surface. These decrease the surface albedo and increase surface absorption of incoming radiation. The insulating effect results from thinning of the sea ice and overlying snow: in the winter, sea ice and snow insulate the relatively warmer ocean from the colder atmosphere. As sea ice and snow thin, more heat can be conducted through the sea ice to the atmosphere, influencing the ice-atmosphere exchange. Thinning ice and snow and increasing conductive heat fluxes can also lead to increased basal sea ice growth – a feedback in a warming world that is seen temporarily in climate projections before warming temperatures overwhelm this feedback and ice growth declines (e.g. Petty et al., 2018; Keen et al, 2020).

30 A large body of previous research has investigated the interactions between sea ice loss and AA. Most of the published research and many of the planned Polar Amplification Model Intercomparison Project (PAMIP) experiments focus on the influence of changes in sea ice concentration (SIC) on Arctic warming (e.g. Peings & Magnusdottir, 2014; Sun et al., 2015; Smith et al.,



2019; Sun et al., 2015). Less attention has been paid to the influence of winter sea ice thinning on Arctic surface warming, in part because observations of sea ice thickness (SIT) have only recently become more readily available, and in part because the effects of SIC losses tend to be large compared to those from SIT changes. Although wintertime SIC in the central Arctic remain high and have changed very little over the satellite era, the sea ice has thinned dramatically (e.g. Kwok and Rothrock, 35 2009; Kwok, 2018). Sea ice volume has decreased by roughly 66% since submarines have been measuring (1958-1976) – and by 50% since 1999 (Kwok, 2018; Lindsay and Schweiger, 2015).

Recent work with atmosphere-only models over both the historical time period and future scenarios suggest that the atmospheric response to SIT changes are strongest in the cold season and at the surface, with atmospheric responses to SIT 40 changes of similar or smaller magnitudes than the responses to SIC changes (e.g. Gerdes, 2006; Krinner, 2010; Lang et al., 2017; Labe et al., 2018; Sun et al., 2017). There is qualitative agreement that the inclusion of SIT changes along with SIC changes leads to an enhancement of surface AA, although the range across different studies is large: two studies focused on late 20<sup>th</sup>-early 21<sup>st</sup> century found annual AA enhanced by ~37-50% with the inclusion of SIT (Lang et al., 2018; Sun et al., 2017), whereas the increase was ~10% in the future simulations (2051-2080) of Labe et al. (2018).

45 Our understanding of the influence of SIT on winter surface AA is further complicated by the presence of snow on sea ice, as well as the heterogeneous distribution of both snow and sea ice thickness. Snow is a more effective insulator than sea ice – and relatively small changes in snow thicknesses can result in large changes in conductive heat fluxes through the ice with consequent impacts on ice-atmosphere exchange. To our knowledge, there have been relatively few basin-scale studies on the 50 effects of snow-on-sea-ice on the winter surface heat budgets in the Arctic in a changing climate. Previous work investigating SIT changes on winter Arctic warming have not typically considered the effects of changing snow cover and often exclude this in the experimental design. For example, Lang et al., (2018) used atmosphere only models that do not allow snow to accumulate on sea ice. Furthermore, previous work with atmosphere-only models specifies grid-cell averaged values for SIT, thus calculating conductive fluxes (which are inversely related to sea ice and snow thicknesses) from an average SIT rather 55 than as a sum over a sub-gridscale thickness distribution. This introduces errors relative to fully-coupled model simulations which typically include a treatment of subgridscale ice thickness variations. These sources of errors and uncertainties also apply to global reanalysis products, most of which use constant sea ice thicknesses and no snow on sea ice for their product estimates (e.g. Wang et al., 2019) and show particularly large errors over the Arctic Ocean (Bromwich et al., 2018; Jakobson et al., 2012 and references therein).

60 In this study we investigate the influence of SIT, snow thickness and heterogeneity in these fields on the Arctic winter energy budget in the climate modeling environment. We explore how projected thickness changes in both sea ice and snow influence conductive heat fluxes and ice-atmosphere heat exchange. We further investigate the importance of heterogeneity in sea ice and snow thicknesses at a model sub-gridcell level, how this impacts conductive heat flux calculations, and quantify the errors



65 that are introduced by using grid-cell average SITs rather than heterogeneous fields. We explore how the wintertime Arctic  
heat fluxes change during a time period (1950-2070) when winter Arctic basin SICs remain high while ice and snow show  
dramatic thinning. This allows us to elucidate the dynamic nature of the influence of sea ice and snow thicknesses on surface  
heat budget even when SIC change is small.

## 2 Models and Analysis

### 70 2.1 CESM1-LE

We use the Community Earth System Model version 1 Large Ensemble (CESM1-LE; Kay et al., 2015) to explore relationships  
between Arctic wintertime conductive heat fluxes and sea ice and snow thickness fields. The CESM1-LE consists of 40  
simulations forced with historical forcing from 1920-2005, and then the Representative Concentration Pathway 8.5 (RCP8.5)  
75 forcing from 2005-2100 (the no-mitigation scenario with a top of the atmosphere radiative forcing of 8.5 W/m<sup>2</sup> by 2100;  
Meinshausen et al., 2011). The sea ice model component (CICE; Hunke et al., 2015) in the CESM1 uses a sub-gridscale ice  
thickness distribution (ITD) in which thermodynamics are calculated over 5 discrete sub-gridcell thickness categories with  
minimum thicknesses of 0., 0.64, 1.39, 2.47 and 4.57 meters. The presence of the ITD influences both the mean climate state  
and climate feedbacks (Holland et al., 2006). The simulated ITD is influenced by ice growth and melt, by ridging due to  
mechanical forcing, and by ice transport (e.g. Thorndike et al., 1975). Snowfall can accumulate on sea ice and be affected by  
80 snow melt, ice ridging and transport. Effectively this means that a different snow depth is present across the different ice  
thickness categories. Ice-atmosphere fluxes are calculated separately in each sea ice thickness category, weighted by the  
concentration in each category, and passed to the flux coupler for use in the atmospheric model. CICE uses a multi-layer  
thermodynamic scheme (Bitz and Lipscomb, 1999; “BL99”) that includes the effects of a prescribed vertical salinity profile.

### 2.2 0-layer thermodynamic conductive heat-flux model

85 Not all thermodynamic variables for individual ice thickness categories were saved as part of the CESM1-LE output. In order  
to disentangle the relative influences of sea ice and snow thicknesses and their distributions, we use the available CESM1 output  
along with the 0-layer thermodynamic model of Semtner (1976) to estimate the conductive heat flux. This simple 0-layer  
model – developed originally to minimize computational costs associated with ice thickness calculations in climate models –  
assumes a linear temperature gradient through the sea ice and snow, and that the conductive heat flux through the ice+snow  
90 layer is:

$$F_{cond} = \frac{Ks(T_b - T_s)}{hs + Ks \left( \frac{SIT}{Ki} \right)}$$

where



$K_s, K_i$  = snow and ice conductivities of heat ( $0.3 \text{ Wm}^{-1}\text{degK}^{-1}$ ,  $2.0 \text{ Wm}^{-1}\text{degK}^{-1}$ )

95  $h_s, SIT$  = snow and ice thicknesses

$T_b, T_s$  = temperatures at the bottom (ocean-ice) and surface (ice-atmosphere) of the ice

This reduces to:

$$F_{cond} = \frac{Ki(T_b - T_s)}{heff}$$

100 where

$heff = (SIT + (K_{ratio} * h_s))$  is a measure of the effective thickness from an insulating perspective, and

$K_{ratio} = K_i/K_s$

In the Arctic winter, surface temperatures remain below the melting point of ice and snow, and the net surface energy budget  
105 (the sum of the net short- and longwave radiation, and sensible and latent heat fluxes) is balanced by the conductive heat flux  
from the ocean through the sea-ice and snow. Climate simulations that prescribe constant sea ice thickness such as those used  
in Atmospheric Model Intercomparison Project (AMIP) and many of the Polar Amplification Model Intercomparison Project  
(PAMIP; Smith et al., 2018) experiments only allow for changes in conductive heat fluxes to occur through changes in  
temperatures and possibly through snow depth changes resulting from changing snowfall. Given this, as the surface  
110 temperature warms, the temperature gradient through the ice decreases, and the conductive heat flux must then decrease (e.g.  
Supplementary material). However, when sea ice and snow thicknesses are allowed to change, these changes can lead to  
increases in conductive heat fluxes despite decreases in the temperature gradient. For example, the conductive heat flux for 2  
m of sea ice with 10 cm of snow and a base-to-surface ice temperature difference of  $40^\circ\text{K}$  is  $30 \text{ W/m}^2$ . This flux is reduced by  
50% - to  $15 \text{ W/m}^2$  - in a warming climate when the temperature difference is reduced to  $20^\circ\text{K}$  and  $SIT$  and  $h_s$  remain the  
115 same. On the other hand, if sea ice and snow thin in the warming climate to a  $SIT$  of 0.5 m and  $h_s$  of 2 cm, the heat flux  
conduction is more than doubled to  $63 \text{ W/m}^2$ . These are not insignificant contributions to the surface energy budget - the two  
single largest terms in the wintertime Arctic ocean surface energy budget are upward and downward longwave radiation,  
typically on the order of  $150\text{-}200 \text{ W/m}^2$  (Huwald et al., 2005). Notably, many simulations that have been used to diagnose  
Arctic Amplification rely on AMIP-type simulations which neglect ice thickness changes (e.g. Smith et al., 2019). Even when  
120 ice thickness anomalies are applied (e.g. Lang et al. 2017; Labe et al. 2018; Sun et al., 2017; Smith et al., 2019), they are  
specified for a mean gridcell value, missing the potential role of ice thickness heterogeneity which could be important given  
that the conductive flux has a non-linear dependence on ice and snow thickness.

### 2.3 Analysis

We are interested in wintertime Arctic heat fluxes during a period when wintertime central Arctic SIC remain relatively high  
125 (1950-2070). We first focus on the month of February to explore in detail relationships between conductive heat fluxes, snow



and sea ice thicknesses, and thickness distributions. Timeseries presented are area averages over the Arctic Ocean ( $68^{\circ}$ - $90^{\circ}$ N from  $100^{\circ}$ - $243^{\circ}$ E, and  $80^{\circ}$ - $90^{\circ}$ N elsewhere – see inset in Fig. 1b), thereby reducing the influence of changes in winter sea ice concentrations (SIC) that are seen in the simulations during this time period in the marginal seas.

130 The model conductive heat flux is available on a gridcell level. It is computed as an area weighted average of the sub-gridcell  
conductive heat fluxes and explicitly accounts for changing ice and snow thicknesses and surface temperatures across the  
different ice thickness categories. Although sub-gridcell conductive heat flux information that would enable us to directly  
relate changes in the sub-gridcell ITD to the net flux was not saved and is not available, sub-gridcell ice and snow thicknesses  
are available. Comparisons between the model net gridcell conductive heat fluxes to those calculated using the sub-gridcell  
135 ice and snow thicknesses, the gridcell surface temperatures and the 0-layer model demonstrate that the 0-layer model gives a  
good approximation for this analysis (Supplemental material). We then compare model conductive heat fluxes which account  
for the subgridscale ice thickness distribution (“CESM-CICE”) with those calculated from the gridcell mean SIT and snow  
thicknesses using the 0-layer model (“MNthick”) to investigate the influence of heterogeneity on conductive heat flux  
calculations.

140

We then explore the relative and changing importance of sea ice conductive heat fluxes to the total surface heat fluxes in a  
warming world in the cold season (October through March) in the 21<sup>st</sup> century. In the high-latitude Arctic winter, when there  
is no solar radiation and the surface air temperature is well below the freezing point, the net surface heat flux over the sea ice  
(total surface short- and longwave radiation, and sensible and latent heat fluxes) is balanced by the conductive heat flux through  
145 the ice and snow. In regions not 100% covered by sea ice, there will also be heat flux from the ocean to the atmosphere. The  
relative contributions of heat fluxes from ocean and sea ice areas will change both as ice and snow thin, and as sea ice  
concentrations decrease. We ask how these relative contributions change in winter months as the projected climate warms.

### 3 Results

#### 3.1 Sea ice and snow thicknesses

150 Over the Arctic Ocean, simulated February surface temperatures and conductive heat fluxes, which are equivalent to the ice-  
atmosphere heat exchange, increase by  $\sim 8^{\circ}\text{C}$  and  $9 \text{ W/m}^2$  between the late 20<sup>th</sup> century and 2070 in the CESM1-LE (Fig. 1a).  
Ocean-ice heat flux increases during this time as well – however by less than  $1 \text{ W/m}^2$  and therefore is not a large contribution  
to the increased net surface heat exchange. Increases in conductive heat flux are driven by decreases in sea ice and snow  
thickness, since the increase in surface temperatures alone would result in a decrease in conductive heat fluxes (Equation 1).  
155 During this time, sea ice concentrations in the Arctic Ocean remain high yet sea ice and snow thin dramatically (Fig. 1b), with  
a mean total effective thickness ( $h_{\text{eff}}$ ) decreasing from a peak near 6 m in the 1970s to 1.5 m by 2070 (Fig. 1c). Snow  
thicknesses averaged over the Arctic Ocean region are typically less than 0.5 m thick – much thinner than sea ice, however



snow – and changes in snow – make significant contributions to both the total effective thickness and the changes in total effective thickness, due to the much larger insulating capacity of snow (Fig. 1c).

160 Conductive heat fluxes increase first over the East Siberian and Chukchi seas (Fig. 2). By the 2050s, increases in conductive heat fluxes of 9-12 W/m<sup>2</sup> are seen not only in the Chukchi and East Siberian seas, but also extending into the Beaufort Sea and the Central Arctic Ocean. Surface temperature increases likewise show the earliest and greatest increases on the Pacific side of the Arctic Ocean. However, by the 2050s the areas of greatest warming (>10°C) are present over comparatively larger sections of the Arctic Ocean, Beaufort Sea and extend as far as northern Greenland. Sea ice concentrations remain above 95%  
165 in the Arctic ocean even by the 2050s – changes in heat fluxes from the relatively warmer ocean to the colder atmosphere are primarily resulting from thinning sea ice and snow rather than increases in open water (see section 3.3). Changes in sea ice thicknesses in the CESM1-LE tend to be largest from the Canadian Archipelago, across the Central Arctic ocean and on to the East Siberian sea (Supplemental material), whereas changes in snow thickness are greatest near the Canadian Archipelago and northern and eastern Greenland. Changes in both sea ice and snow thicknesses are important contributors to the changes in  
170 effective thickness (Fig. 2). Although snow depth changes are small compared to changes in SIT, they contribute 40% or more to the changes in effective thicknesses from the central Arctic Ocean to the Canadian Archipelago, Greenland and into the Atlantic sector of the Arctic ocean (Fig. 2 and Supplemental material). It is important to note that changes in conductive heat fluxes during this time are mitigated by changes in surface temperatures: the roughly 13° surface warming over this period would lead to ~5 W/m<sup>2</sup> decrease in conductive heat flux if the sea ice and snow did not thin.

### 175 3.2. Sea ice and snow thickness distributions

We investigate the influence of thickness distributions on conductive heat fluxes by calculating conductive heat fluxes using the Semtner 0-layer model, daily mean sea ice and snow thicknesses over the ice-covered areas in each grid cell along with daily gridcell average surface temperatures (“MNthick”), and then averaging over the month of February. Relative to the fluxes computed by the full model (CESM-CICE), the MNthick conductive heat fluxes underestimate heat fluxes throughout the  
180 Arctic Ocean (Fig. 3a, and Supplemental material). Ensemble mean Arctic Ocean average conductive heat flux is underestimated by ~6-9 W/m<sup>2</sup> using MNthick (Fig. 3). This highlights the importance of resolving thin ice and snow within the subgridscale ice thickness distribution.

Differences between these winter-time conductive heat fluxes throughout the Arctic basin are larger in the beginning of the  
185 21<sup>st</sup> century (by ~35%) when considerable thick ice is present. Discrepancies between MNthick conductive heat fluxes and CESM-CICE are small by the 2070s (~16%) when almost all the February sea ice in the Arctic Ocean has thinned considerably and the ITD lies within the two thinnest sea ice categories (Fig. 3c). Although grid-cell average thicknesses lead to an underestimation of mean conductive heat fluxes, they result in an overestimation in the changes in conductive heat fluxes (by ~36% by 2070; Fig. 3b) and thus influence feedbacks in the warming climate.

190



3.3 Relative contributions of conductive heat flux changes to total surface heat flux changes in a warming climate  
SICs in the wintertime high latitude central Arctic ocean ( $80^{\circ}$ - $90^{\circ}$ N) start falling below 90% first in October (2020s), and by  
2070 SICs are below 90% even for December, although they remain above 90% for January through March (Fig. 4). Although  
SICs change very little over this time period in the latter winter months (Dec-Mar), sea ice thins markedly and by 2070 the  
195 ensemble average SIT is less than 1m for all winter months (not shown). Changes in surface temperatures (Fig. 4a) and heat  
fluxes (Fig. 4b) are larger when SICs fall below 90% and more open water is exposed, yet significant increases in both surface  
temperatures ( $\sim 16^{\circ}\text{C}$ ) and heat fluxes ( $\sim 20\text{W}/\text{m}^2$ ) occur even while SICs remain high. Increases in the conductive heat flux  
associated with the thinning of ice and snow contribute  $\sim 50\%$ - $80\%$  or more of the changes in the net surface heat fluxes when  
the SICs are above  $\sim 90\%$ - $98\%$  (Fig. 4c).

#### 200 4 Discussion and Conclusions

This analysis has important implications for atmosphere-only simulations and reanalysis products that require specified sea  
ice concentrations, sea ice thicknesses and snow depths for boundary conditions. These simulations typically prescribe changes  
in sea ice concentration but neglect changes in ice and snow thickness. The sea ice concentration changes lead to large changes  
in albedos, and also direct ocean-atmosphere heat fluxes as more ocean water is exposed to the atmosphere. However, by  
205 neglecting changes in ice and snow thickness, the changing insulating effect of sea ice is missing. As the climate warms,  
changing winter Arctic surface heat fluxes will be dominated by this insulating effect and resulting changes in conductive heat  
fluxes until the sea ice thins enough or SICs decrease enough such that direct ocean-atmosphere heat fluxes become more  
important. In the CESM1-LE, with changing subgridscale ice and snow thicknesses, conductive heat fluxes contribute over  
half of the Dec-Mar surface heat fluxes until 2050-2070. Atmosphere only simulations that consider only changes in sea ice  
210 concentrations and ignore changes in sea ice and snow thicknesses will simulate that the winter atmosphere in high ice  
concentration regions gains less heat from the surface under climate warming. However, if changing ice and snow depths are  
accounted for, the conductive heat fluxes increase and the atmosphere is warmed more. In the CESM1-LE, Arctic basin  
conductive heat flux increases by  $\sim 8\text{-}10\text{ W}/\text{m}^2$  from 2000 to 2070 as winter SIC remain above 90%.

215 Sea ice and snow exhibit high spatial heterogeneity and climate models often account for this through the inclusion of a  
subgridscale ice thickness distribution within their sea ice treatment. This heterogeneity of both sea ice and snow fields impacts  
conductive heat fluxes and thus the projected changes in the net surface heat flux. Climate models that calculate sea ice  
thermodynamics over only gridcell mean sea ice and snow thicknesses (for example in AMIP style simulations) will both  
underestimate mean wintertime conductive heat fluxes, as well as overestimate changes in conductive heat fluxes as the ice  
220 thins during periods of time that the sea ice goes from relatively thick to relatively thin. These differences can be significant –  
in the CESM1-LE mean conductive heat fluxes calculated using grid-cell mean thicknesses lead to an underestimation of  $\sim 16\text{-}$



35% in mean values and an overestimation of up to ~36% in the changes in conductive heat fluxes in the wintertime Arctic basin even while SIC remain above 90%.

225 These results highlighting the transient nature of the influences of SIT, snow thicknesses, and their distributions on wintertime surface heat budgets in the CESM suggest that errors due to calculations of conductive heat fluxes in climate models (including atmosphere-only simulations) may depend on the initial model mean state. The thermodynamics of sea ice are dependent on the mean ice state (e.g. Massonnet et al., 2018) – and this has important implications not only for sea ice evolution in a changing world, but also surface heat fluxes in ice covered areas. Models with a relatively thin sea ice mean state will have higher errors  
230 in changes in surface heat fluxes depending on whether they use grid-cell mean SITs or heterogeneous fields. Sea ice and snow on sea ice are important components of polar climate thermodynamics and their dynamic and heterogeneous nature – although complicated – play important roles in surface heat budgets.

Snow is a much more effective insulator than sea ice and plays important roles in sea ice mass budgets and climate feedbacks.  
235 Snow depths and distributions in the CESM1-LE are roughly equally important contributors as sea ice thicknesses and distributions on wintertime conductive heat fluxes. Snow depth distributions in the CESM1-LE show similar patterns compared to observations across the Arctic Basin, although simulated snow depths tend to be more evenly distributed and thicker than observed (Webster et al., 2020). Snow thicknesses in the most recent version of CESM – the CESM2 – tend to be underestimated and have low variability compared to observations. These differences between simulations are due largely to  
240 differences in precipitation and the mean sea ice state in these two models (Webster, et al., 2020). Discrepancies between simulations and observations, however, are not well understood and suggest that future collaborative work to test and improve snow distributions in the modeling environment would be important for increasing our understanding of Arctic climate and predicting snow impacts in a warming climate.

### Code and Data availability

245 All analysis and figures were completed using the NCAR Command Language (The NCAR Command Language v.6.6.2 (UCAR, NCAR, CISL and TDD,2019); <https://doi.org/10.5065/D6WD3XH5>). The scripts used to perform the analysis and generate the figures in this manuscript are available on GitHub ([https://github.com/llandrum/Cryosphere\\_SeaIce\\_Snow\\_Thicknesses\\_ArcticHeatFlux](https://github.com/llandrum/Cryosphere_SeaIce_Snow_Thicknesses_ArcticHeatFlux)) and archived in Zenodo (Landrum, 2021). The CESM-LE data are freely available from the following link: <http://www.cesm.ucar.edu/projects/community-projects/LENS/> (last access: 7 April 2020, Deser and Kay, 2020; Kay et al., 2015).  
250





### Author contribution

LL and MMH formulated the research goals and questions. LL made the figures and performed the analysis with input from MMH. LL prepared the manuscript with contributions from MMH.

### 255 Competing interests

The authors declare that they have no conflict of interest.

### Acknowledgments

We acknowledge funding from NSF-OPP 1724748. We also acknowledge the CESM Large Ensemble Community Project and supercomputing resources (doi:10.5065/D6RX99HX) provided by the Climate Simulation Laboratory at NCAR's  
260 Computational and Information Systems Laboratory, sponsored by the National Science Foundation and other agencies.

We thank Alice DuVivier for providing the daily CESM1-TS data so that we could compare 0-layer to multi-layer model estimates of conductive heat fluxes

### References

- Bitz, C. M. and Lipscomb, W. H.: An energy-conserving thermodynamic sea ice model for climate study. *J. Geophys. Res.-*  
265 *Oceans*, **104(C7)**, 15,669–15,677, <https://doi.org/10.1029/1999JC900100>, 1999.
- Bromwich, D., and Coauthors: The Arctic System Reanalysis, version 2. *Bull. Amer. Meteor. Soc.*, **99**, 805–828, <https://doi.org/10.1175/BAMS-D-16-0215.1>, 2018.
- Dai, A., Luo, D., Song, M. and Liu, J.: Arctic amplification is caused by sea-ice loss under increasing CO<sub>2</sub>. *Nat Commun* **10**, 121. <https://doi.org/10.1038/s41467-018-07954-9>, 2019.
- 270 Deser, C. and Kay, J. E.: CESM Large Ensemble Community Project, available at: <http://www.cesm.ucar.edu/projects/community-projects/LENS/>, last access: 7 April, 2020.
- European Centre for Medium-Range Weather Forecasts (ECMWF): IFS documentation–CY41R2. part IV: physical processes, doi: [10.21957/tr5rv27xu](https://doi.org/10.21957/tr5rv27xu) [Available at <https://www.ecmwf.int/en/elibrary/16648-ifs-documentation-cy41r2-part-iv-physical-processes>, accessed 03.29.2021.], 2016.
- 275 Feldl, N., Po-Chedley, S., Singh, H. K. A., Hay, S., and Kushner, P. J.: Sea ice and atmospheric circulation shape the high-latitude lapse rate feedback, *Nature Partner Journals Climate and Atmospheric Science*, **3**, 41, doi.org/10.1038/s41612-020-00146-7, 2020.



- Gates, W. L., Boyle, J., Covey, C., Dease, C., Doutriaux, C., Drach, R., Fiorino, M., Gleckler, P., Hnilo, J., Marlais, S., Phillips, T., Potter, G., Santer, B., Sperber, K., Taylor, K. and Williams, D.: An Overview of the Results of the Atmospheric Model Intercomparison Project (AMIP I). *Bull. Amer. Meteor. Soc.*, **73**, 1962-1970 (1998).
- 280 Gerdes, R.: Atmospheric response to changes in Arctic sea ice thickness. *Geophysical Research Letters*, **33**, L18709. <https://doi.org/10.1029/2006GL027146>, 2006.
- Graversen, R. G. and Wang, M.: Polar amplification in a coupled climate model with locked albedo, *Clim. Dynam.*, **33**, 629–643, 2009.
- 285 Hall, A.: The role of surface albedo feedback in climate, *J. Clim.*, **17**, 1550–1568, 2004.
- Holland, M. M. and Bitz, C. M.: Polar amplification of climate change in coupled models. *Clim. Dyn.* **21**, 221-232. Doi: 10.1007/s00382-003-0332-6, 2003.
- Hunke, E. C., Lipscomb, W. H., Turner, A. K., Jeffery, N., and Elliot, S.: CICE: the Los Alamos Sea Ice Model Documentation and Software User’s Manual Version 5.1, LA-CC-06-012., 2015.
- 290 Huwald H., Tremblay, L. B., and Blatter, H.: Reconciling different observational data sets from Surface Heat Budget of the Arctic Ocean (SHEBA) for model validation purposes. *J Geophys Res* 110:C05009. doi:10.1029/2003JC002221, 2005.
- Kay, J. E. and Coauthors: The Community Earth System Model (CESM) Large Ensemble Project: a community resource for studying climate change in the presence of internal climate variability. *Bull. Am. Meteorol. Soc.* **96**, 1333–1349, 2015.
- Keen, A. and Coauthors: An inter-comparison of the mass budget of the Arctic sea ice in CMIP6 models. *The Cryosphere*,  
295 <https://doi.org/10.5194/tc-2019-314>, 2020.
- Kumar, A., Perlwitz, J., Eischeid, J., Quan, X., Xu, T., Zhang, T., Hoerling, M., Jha, B., and Wang, W.: Contribution of sea ice loss to Arctic amplification, *Geophys. Res. Lett.*, **37**, L21701, doi:10.1029/2010GL045022, 2010.
- Kwok, R.: Arctic sea ice thickness, volume, and multiyear ice coverage: losses and coupled variability (1958-2018), *Environ. Res. Lett.*, **13**, 105005, 2018.
- 300 Jakobson, E., Vihma, T., Palo, T., Jakobson, L., Keernik, H., and Jaagus, J.: Validation of atmospheric reanalyses over the central Arctic Ocean. *Geophys. Res. Lett.*, **39**, L10802, <https://doi.org/10.1029/2012GL051591>, 2012.
- Labe, Z.M., Peings, Y and Magnusdottir, G.: Contributions of ice thickness to the atmospheric response from projected Arctic sea ice loss, *Geophys. Res. Letters*, DOI:10.1029/2018GL078158, 2018.
- Landrum, L. Scripts for figures and analysis for “Influences of changing sea ice and snow thicknesses on winter Arctic heat  
305 fluxes”. Zenodo <https://doi.org/10.5281/zenodo.5161076>, 2021.
- Lang, A., Yang, S. and Kaas, E.: Sea ice thickness and recent Arctic warming. *Geophys. Res. Lett.*, **44**, 409–418, <https://doi.org/10.1002/2016GL071274>, 2017.
- Laxon, S. W., and Coauthors: CryoSat-2 estimates of Arctic sea ice thickness and volume. *Geophys. Res. Lett.*, **40**, 732–737, <https://doi.org/10.1002/grl.50193>, 2013.
- 310 Lindsay, R., and Schweiger, A.: Arctic sea ice thickness loss determined using subsurface, aircraft, and satellite observations. *The Cryosphere*, 9(1), 269–283. doi:10.5194/tc-9-269-2015, 2015.



- Massonnet, F., Vancoppenolle, M., Goosse, H. and Coauthors: Arctic sea-ice change tied to its mean state through thermodynamic processes. *Nature Clim Change* **8**, 599–603, <https://doi.org/10.1038/s41558-018-0204-z>, 2018.
- Meinshausen, M., Smith, S. J., Calvin, K. and Coauthors: The RCP greenhouse gas concentrations and their extensions from 1765 to 2300. *Climatic Change* **109**, 213 doi:10.1007/s10584-011-0156-z, 2011.
- 315 Peings, Y., and G. Magnusdottir, G.: Response of the wintertime Northern Hemisphere atmospheric circulation to current and projected Arctic sea ice decline: A numerical study with CAM5. *Journal of Climate*, **27**(1), 244–264. <https://10.1175/JCLI-D-13-00272.1>, 2014.
- Petty, A. A., Holland, M. M., Bailey, D. A. and Kurtz, N T.: Warm Arctic, increased winter sea ice growth? *Geophys. Res. Lett.*, **45** (23), 12,922–12,930, <https://doi.org/10.1029/2018GL079223>, 2018.
- 320 Pithan, F. and Mauritsen, T.: Arctic amplification dominated by temperature feedbacks in contemporary climate models. *Nat. Geosci.* **7**, 181–184, 2014.
- Screen, J. A. and Simmonds, I.: The central role of diminishing sea-ice in recent Arctic temperature amplification. *Nature* **464**, 1334–1337, 2010.
- 325 Screen, J. A., Simmonds, I., Deser, C., and Tomas, R.: The atmospheric response to three decades of observed Arctic sea ice loss, *J. Clim.*, **26**(4), 1230–1248, doi:10.1175/JCLI-D-12-00063.1, 2013.
- Screen, J. A. and Coauthors: Consistency and discrepancy in the atmospheric response to Arctic sea-ice loss across climate models. *Nat. Geoscience* **11**(3), 155–163, <https://doi.org/10.1038/s41561-018-0059-y>, 2018.
- Serreze, M. C., Barrett, A. P., Stroeve, J. C., Kindig, D. N., and Holland, M. M.: The emergence of surface-based Arctic amplification, *Cryosphere*, **3**(1), 11–19, doi:10.5194/tc-3-11-2009, 2009.
- 330 Serreze, M. C., and Barry, R. G.: Processes and impacts of Arctic amplification: A research synthesis, *Global Planet. Change*, **77**(1), 85–96, doi:10.1016/j.gloplacha.2011.03.004, 2011.
- Serreze, M. C., and Stroeve, J.: Arctic sea ice trends, variability and implications for seasonal ice forecasting. *Philosophical Transactions of the Royal Society of London A: Mathematical, Physical and Engineering Sciences*, **373**(2045), <https://doi.org/10.1098/rsta.2014.0159>, 2015.
- 335 Semtner, A. J.: A Model for the Thermodynamic Growth of Sea Ice in Numerical Investigations of Climate. *J. Phys. Oceanogr.* **6**, 379–389, 1976.
- Smith, D. M., Screen, J. A., Deser, C., Cohen, J., Fyfe, J. C., García-Serrano, J., Jung, T., Kattsov, V., Matei, D., Msadek, R., Peings, Y., Sigmond, M., Ukita, J., Yoon, J.-H. and Zhang, X.: The Polar Amplification Model Intercomparison Project (PAMIP) contribution to CMIP6: investigating the causes and consequences of polar amplification, *Geosci. Model Dev.*, **12**, 1139–1164, <https://doi.org/10.5194/gmd-12-1139-2019>, 2019.
- 340 Sun, L., Allured, D., Hoerling, M., Smith, L., Perlwitz, J., Murray, D. and Eischeid, J.: Drivers of 2016 record Arctic warmth assessed using climate simulations subjected to Factual and Counterfactual forcing. *Weather and Climate Extremes* **19**, doi:10.1016/j.wace.2017.11.001, 2018.



- 345 Sun, L., Deser, C., and Tomas, R. A.: Mechanisms of stratospheric and tropospheric circulation response to projected Arctic sea ice loss\*. *Journal of Climate*, 28, 7824–7845. <https://doi.org/10.1175/JCLI-D-15-0169.1>, 2015.
- Vavrus, S.: The impact of cloud feedbacks on Arctic climate under greenhouse forcing, *J. Clim.*, 17, 603–615, 2004.
- Wang, C., Graham, R. M., Wang, K., Gerland, S., and Granskog, M.: Comparison of ERA5 and ERA-Interim near-surface air temperature, snowfall and precipitation over Arctic sea ice: effects on sea ice thermodynamics and evolution. *Cryosphere*, 13, 1661-1679, <https://doi.org/10.5194/tc-13-1661-2019>, 2019.
- 350 Webster, M. A., DuVivier, A. K., Holland, M. M., and Bailey, D. A.: Snow on Arctic Sea Ice in a Warming Climate as Simulated in CESM. *J. Geophys. Res.: Oceans*, 125, e2020JC016308. <https://doi.org/10.1029/2020JC016308>, 2020.

### Figure captions

**Figure 1.** CESM1-LE February area-averaged Arctic Ocean (a) surface temperatures, oceanic heat fluxes and conductive heat fluxes; (b) SIC, SIT and snow thicknesses ( $h_s$ ); and (c) effective snow thickness ( $K_{ratio} * h_s$ ), and effective total thicknesses (heff). Ensemble means are show in the solid lines, ensemble ranges in opaque polygons. Arctic Ocean region is shown in the map insert in the middle panel.

355

**Figure 2.** February decadal mean changes (from 1950-1959) in surface temperatures (a, d), conductive heat fluxes (b, e), and effective sea ice + snow thickness (heff; e, f) for the 2010s (a, b, c) and 2050s (d, e, f). The 98% SIC for each decade is shown by the thick black contour. Stippled areas in the effective thickness (heff) change figures (c, f) indicate regions where changes in effective snow thickness ( $K_{ratio} * h_s$ ) account for 40% or more of the changes in the total effective thickness (heff = SIT +  $K_{ratio} * h_s$ ).

360

**Figure 3.** CESM1-LE February area-averaged Arctic Ocean (a) mean conductive heat fluxes from the model output (“CESM1-CICE”; dark blue) and calculated from mean ice and snow thicknesses (“MNthick”; light blue), and the ratio of MNthick to CESM1-CICE (red); (b) changes in February conductive heat fluxes; and (c) sea ice areas by thickness category as well as total sea ice area (dark blue). Ensemble means are show in the solid lines, ensemble ranges in opaque polygons. The solid black line in top panel indicates a MNthick:CESM1-CICE conductive heat flux ratio of 0.75 for reference. Ensemble means in middle panel are thick where the differences become statistically significant at the 95% confidence level (2030 onwards).

370

**Figure 4.** High latitude central Arctic ocean (80°-90°N) area averaged cold season (October-March) changes in: surface temperature (a), net surface heat flux (b), and relative contribution of changes in conductive heat flux to the changes in net surface heat flux (c). White dashed/solid contours indicate 98%/90% SIC.

375



### FEB Arctic Ocean

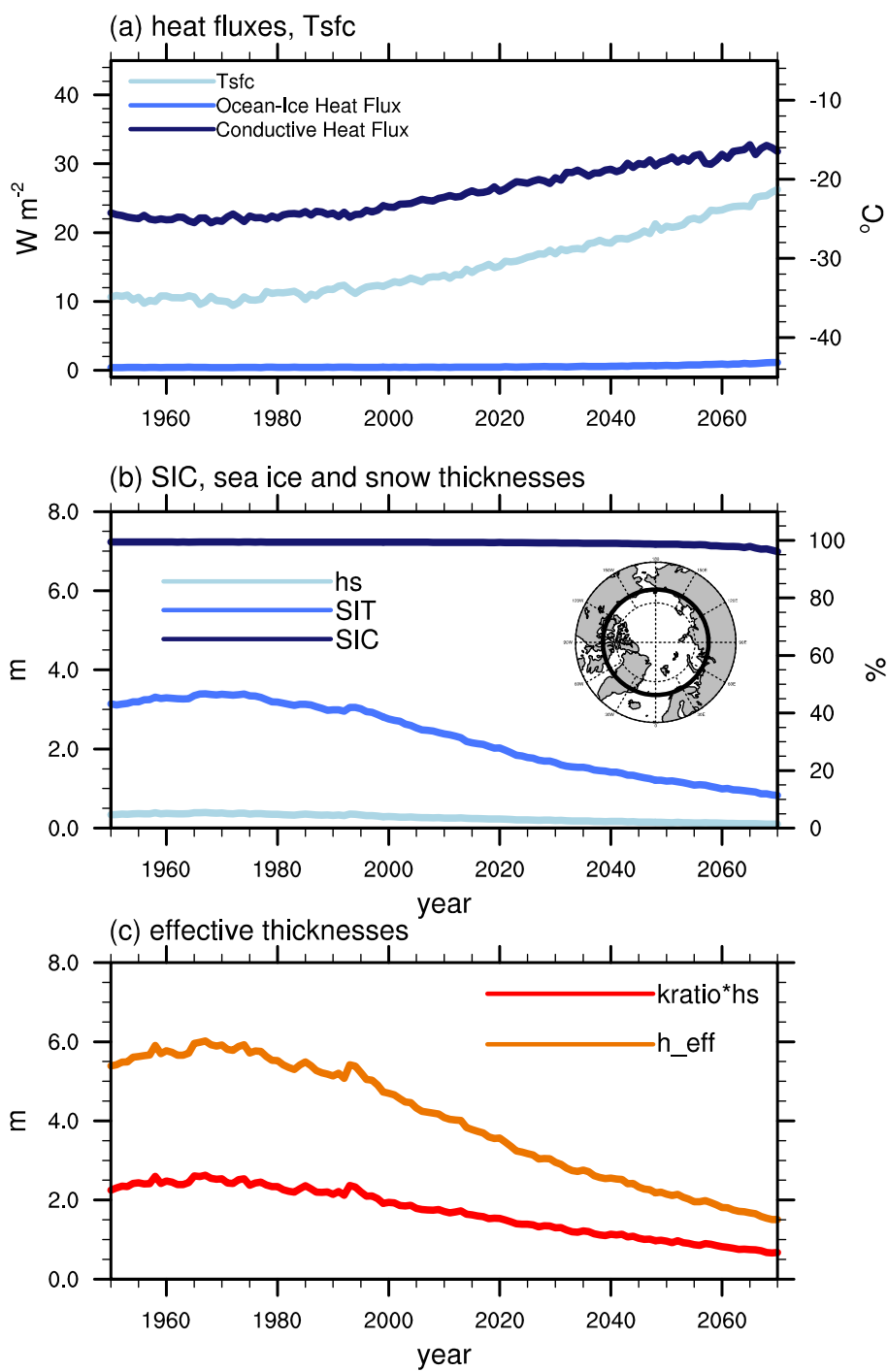


Figure 1

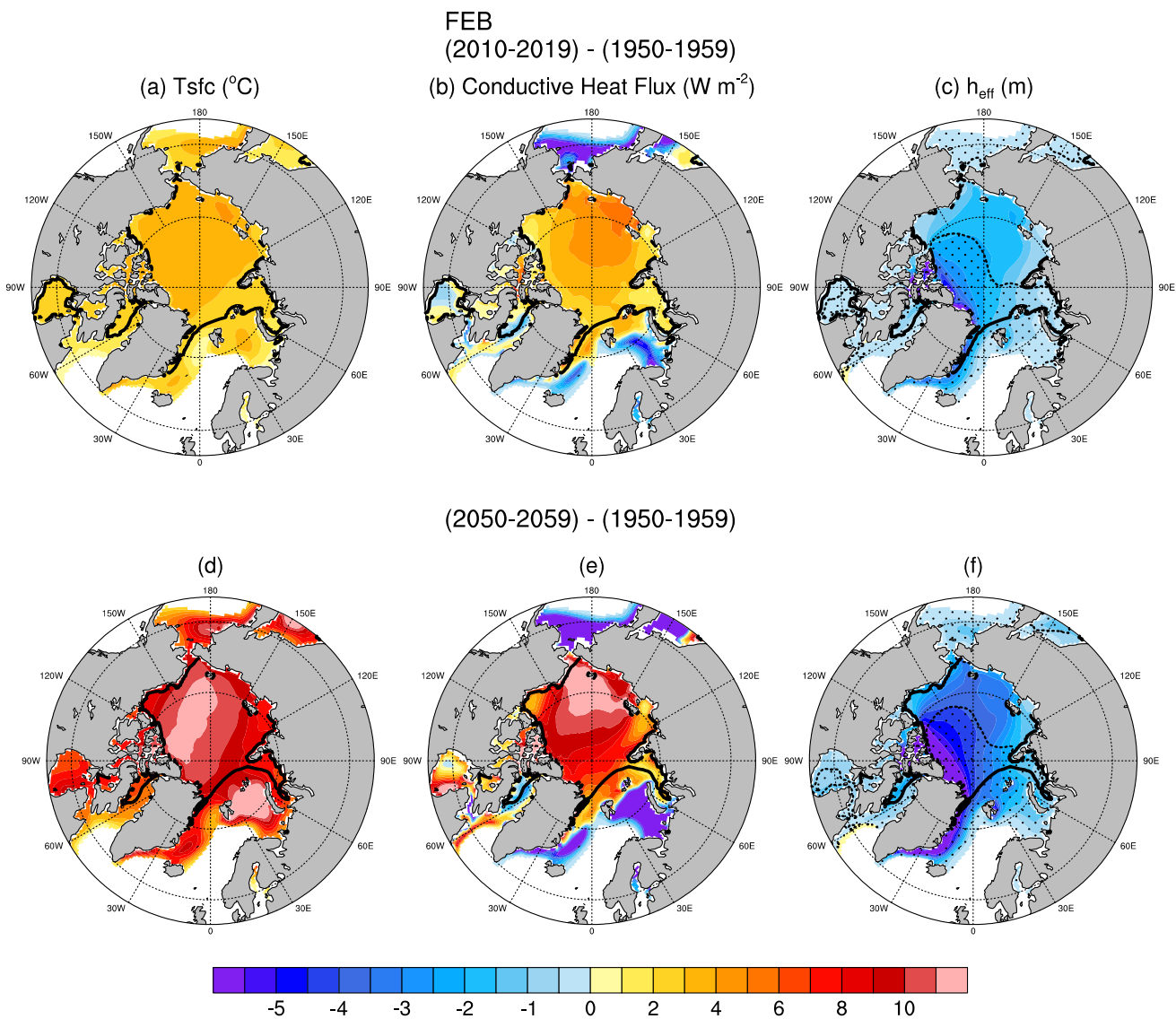


Figure 2

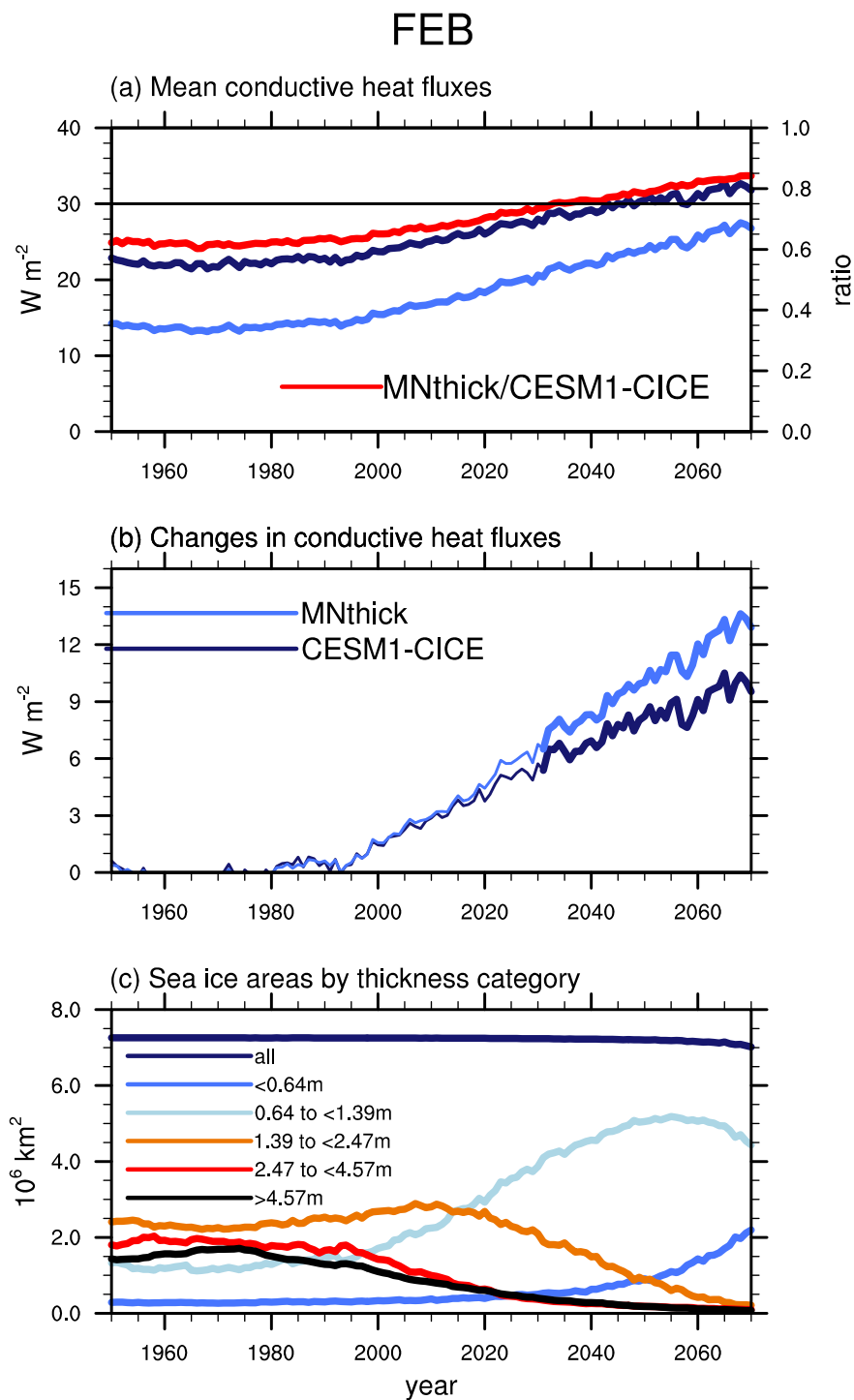


Figure 3

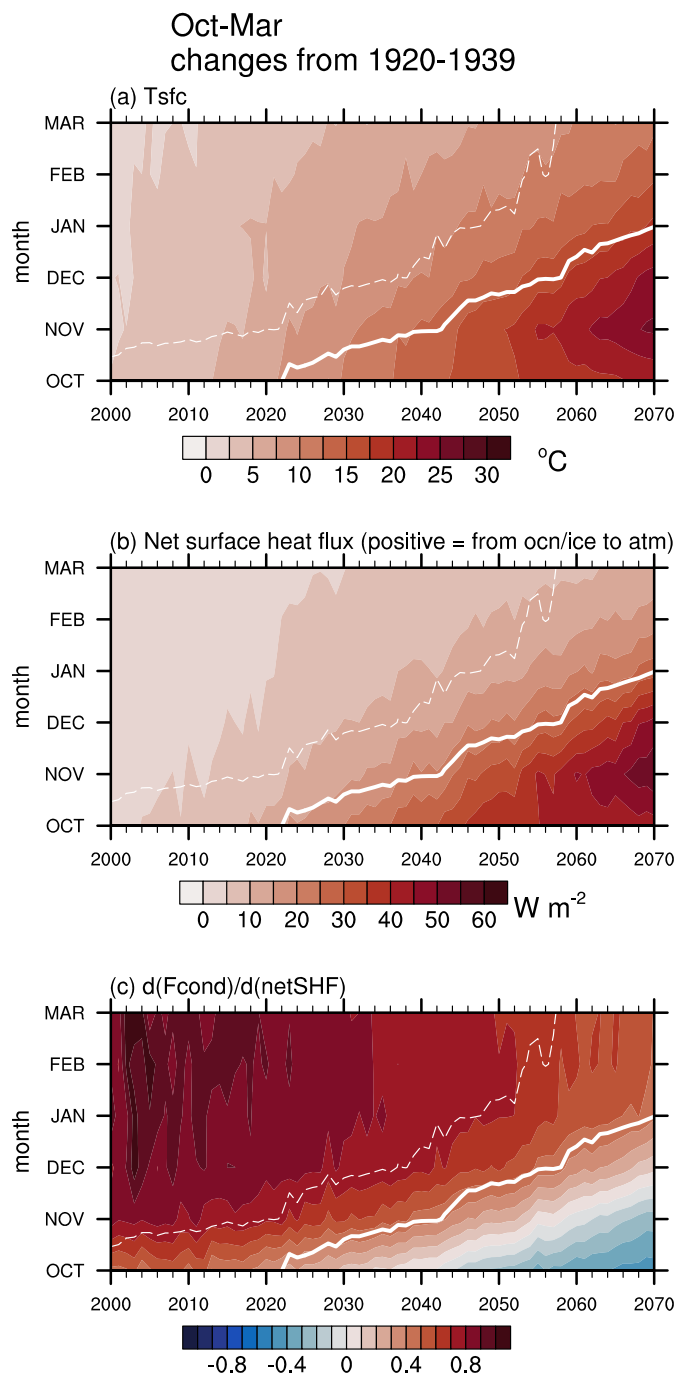


Figure 4